Whole Sky Imagers For Real-Time Cloud Assessment, Cloud Free Line of Sight Determinations and Potential Tactical Applications

Janet E. Shields*, Richard W. Johnson, Monette E. Karr, Art R. Burden, and Justin G. Baker
Marine Physical Lab, Scripps Institution of Oceanography, University of California San Diego,
9500 Gilman Dr., La Jolla CA 92093-0701

ABSTRACT

Whole Sky Imagers (WSI) have been developed at the Marine Physical Lab for several military and research applications over many years. This paper discusses several systems useful for real-time monitoring of cloud conditions and radiance distribution, and for tactical applications. We include a discussion of several data products, including the results of a Cloud Free Line of Sight (CFLOS) statistical study based on an evaluation of approximately 800,000 WSI images.

The Day/Night WSI is the most capable of the WSI systems. It can be remotely sited from a user, and can provide near-real-time assessment of cloud conditions during the day and at night. While each unit is designed for a specific application, output products can include day and night cloud fraction, cloud condition along selected tracks or in moving regions of interest, and the absolute sky radiance distribution. The ability to extract earth-to-space beam transmittance is in development. At the smaller end of the instrument system scale, a light-weight WSI has been developed for use in an Unmanned Aerial Vehicle, which could be modified for tactical use. Data acquired by earlier versions of the WSI's have now been processed to yield CFLOS statistics. The data were acquired at one-minute intervals for over two years at several sites in the late 1980's. CFLOS statistics as a function of location, cloud fraction, and look angle will be presented, along with persistence results. A new tactical optical system in early development uses one or more fisheye lenses to enable a user to view the full surround, with simultaneous high-resolution views of selected regions of interest within the scene. This concept has a patent pending, and we foresee that these capabilities can be used for now-casting of battlefield environmental conditions.

Key words: Cloud, radiance, tactical imager, now-cast, UAV, visible, NIR, CFLOS, cloud persistence, battlefield, whole sky imager

1. OVERVIEW

Whole Sky Imagers (WSI) are ground-based sensors which are used in military test site support, global climate research, UV research, and other applications. They are designed to provide high quality digital imagery of sky conditions and, when combined with appropriate algorithms, provide assessment of cloud amount and location within the scene, absolute radiance distribution, and related atmospheric parameters. The Marine Physical Lab (MPL) at Scripps Institution of Oceanography has been very active in the development of WSI systems for the last two decades. The first WSI systems the group developed using digital imaging technology were deployed in the early 1980's, and were followed by fully automated systems in the mid to late 1980s (Johnson et al 1989, and Shields et al., 1993). WSI systems capable of full 24-hour autonomous operation for acquisition of day and night sky parameters were fielded in the early 90's, and have continued to evolve in capability (Shields et al 1998).

* jshields@ucsd.edu; phone (858) 534-1769; fax (858) 822-0665

This paper will give an overview of the development of the WSI sensors, and then discuss the Day/Night WSI data products in more detail, emphasizing those areas that are applicable to military requirements. Sample Cloud Free Line of Sight (CFLOS) statistics will be presented, including persistence results and multi-station results. These CFLOS statistics were processed for the Starfire Optical Range using the Day WSI data-base. Finally, we will discuss the developmental Tactical Full Scene Imager (with patent pending) which can be used to provide unique imagery for a number of tactical applications and environmental now-casting applications.

2. DEVELOPMENT OF FISHEYE IMAGING SYSTEMS AT MPL

The original concept for the development of calibrated fisheye imaging systems at MPL evolved out of the group's Atmospheric Optics program, a measurement and modeling program using multiple sensors for monitoring sky radiance, atmospheric scattering coefficient profiles, and other parameters related to vision through the atmosphere (Johnson et al., 1980). Beginning in the early 1980's, the group developed a series of ground-based calibrated fisheye imaging systems known as Whole Sky Imagers (WSI) that used digital imagery and were fully automated. The first automated WSI was conceived as combining the features of the all-sky cameras used in earlier programs, with the scanning radiometer systems that provided measurements of sky radiance distribution. The first WSI systems used digital cameras (sometimes CCD, sometimes Charge Injection Device or CID imagers), with fisheye lenses, optical filter changers, relay optics to provide the proper image size and location, equatorial sun occultors to provide shading for the fisheye lens, and early versions of personal computers for automated control. Figure 1 shows some of this evolution. The film-based all-sky camera in use in a 1963 deployment is shown in Figure 1a, and the automated Day-only WSI developed in the early and mid-1980's based on CID technology is shown in Figure 1b. With the use of very low noise 16 bit CCD cameras and an occultor modified to handle both sun and moon, these systems were further developed into the Day/Night WSI shown in Figure 1c. Some typical images from the Day/Night WSI are shown in Figure 2.

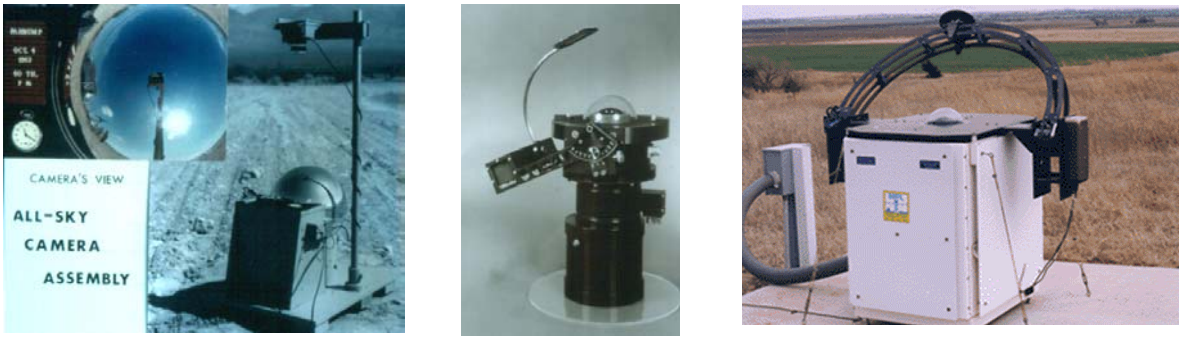

(a) (b) (c)

Figure 1: Some of the WSI Systems developed at MPL that contributed to the development of the Day/Night WSI: a) the All-Sky Camera used in 1963; b) the Day-only WSI used in the 1980's; c) the Day/Night WSI used in 1990's and currently in use.

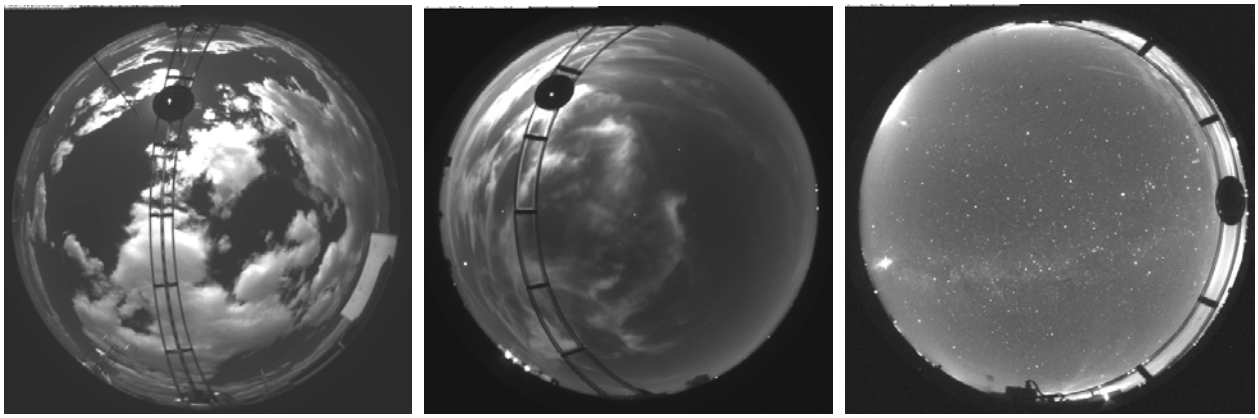

Figure 2: Sample imagery from the Day/Night WSI for sunlight, moonlight, and starlight conditions.

The Day/Night WSI is fully automated, and acquires data continuously 24-hours a day. It has been environmentally hardened, and there are versions of the D/N WSI running in the desert, Arctic, tropics, and other environments. The lens covers the full upper hemisphere, down to just below the horizon (with a field of view of 181.5 degrees typically). The system uses a Series 200 or Series 300 Photometrics 16-bit CCD camera. This camera has a three-stage Peltier cooler on the chip, and is cooled to approximately –40C. The full dynamic range of the WSI system is over 10 logs (a factor of 10^{10}) due to a combination of the dynamic range of the camera, the neutral density offset filters, changes in camera exposure time, and changes in spectral filters. With this dynamic range and low noise camera, the WSI acquires imagery under daylight, moonlight, and starlight; under starlight, even the darkest part of the sky between stars has a signal to noise ratio of 50 or more under most conditions.

A dual-wheel filter changer enables adjusting flux levels with neutral density filters, and changing spectral filters. The spectral filter options are blue (450 nm), red (650 nm), NIR (800 nm) and open hole for use at night. The solar/lunar occultor provides full shading of the front optics, in order to minimize stray light. (A much smaller shade could provide shading such that the sun does not directly illuminate the CCD, however we feel that it is vital, in order to acquire high quality data, to shade the full extent of the front optics.) This of course means that the solar/lunar occultor must be held at a reasonably large distance from the lens so that it does not obscure excessive fractions of the sky dome. A new occultor has recently been designed, which should shade only 2-3% of the upper hemisphere while still shading the full optics.

3. WSI DATA PRODUCTS

The primary WSI data products are the displayed images such as shown in Fig. 3a, the cloud fraction images shown in Fig. 3b, the total cloud fraction and cloud fraction in selected regions of interest, and absolute radiance distribution. The ability to extract earth-to-space beam transmittance at night is also working in its preliminary version. The raw data are automatically converted to an 8-bit display on the computer monitor. This displayed imagery is useful for a number of applications even without further processing. For example, some of our sponsors have used this data to evaluate the sky condition visually during tests, for determining an appropriate window of opportunity for specific tests, and for evaluating conditions along satellite tracks during tests.

A number of current and potential applications require an automated cloud algorithm. These applications include automated analysis of cloud fraction for modeling, automated assessment of cloud conditions in specific regions of the image, and potentially automated alarms. During the daytime, the cloud decision algorithm identifies each pixel as opaque cloud, thin cloud, no cloud, or no data. Results of the daytime cloud algorithm are shown in Figure 3.

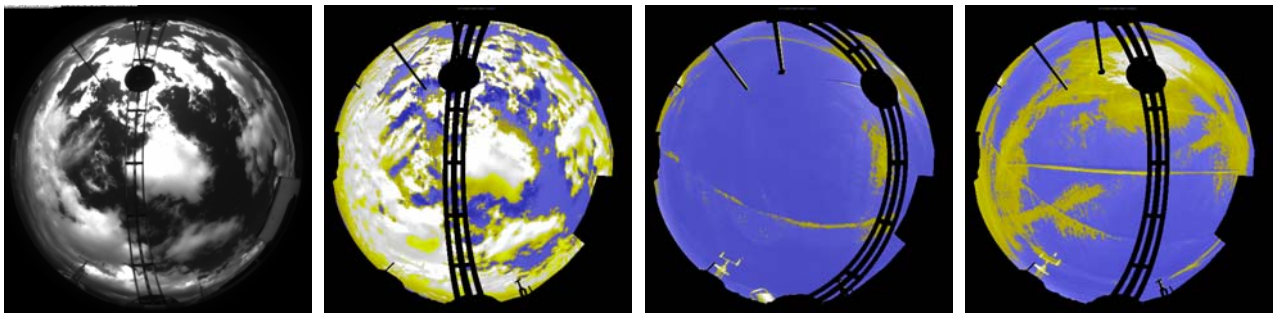

(a) (b) (c) (d)

Figure 3: Day Cloud Algorithm Result: a) Raw data with cumulus or alto-cumulus clouds; b) Cloud decision result for image a, where white is optically opaque, yellow is optically thin, blue is no cloud, and black is no data; c) Cloud decision result for thin clouds associated with contrails; d) Cloud decision result 2 hours after image c.

For opaque clouds, the daytime cloud algorithm is based on the red/blue ratio at each pixel. For thin clouds, it is based on a ratio between the measured red/blue ratio and the pre-determined red/blue ratio for a clear sky for the same solar zenith angle. That is, the thin cloud algorithm takes into account the variation in spectral signature of the sky as a function of look angle and solar zenith angle. The algorithm generally works well for opaque clouds and moderately thin clouds. Under hazy conditions, however, it has difficulty distinguishing very thin clouds from the haze or aerosols. An

upgrade to use the NIR filter data is in development with the Day WSI, and we hope to apply the new work to the Day/Night WSI in the future. It should also be mentioned that DOE's Atmospheric Radiation Measurement (ARM) Program uses an alternative algorithm, which is beyond the scope of this article.

Most of the military D/N WSI systems developed for Starfire Optical Range and other sponsors have the cloud algorithm running in near-real time. These systems also use a first-version night algorithm. A typical night algorithm result is shown in Figure 4. The night algorithm currently uses 357 cells in the sky, and makes an assessment within each cell of the cloud condition. We consider the algorithm result shown in Figure 4 to be somewhat preliminary. It was based on detection of stars from a star library, in conjunction with an angular calibration of the image. The angular calibration is accurate to within approximately half a pixel. For each star, the image is inspected to determine if the star can be detected. If it is detected, the area under the point spread function for the star is evaluated, and a contrast between this integrated signal and the background is determined. The clouds are identified using contrast thresholds that depend on star magnitude, moon phase, and look angle. We would like to update this algorithm using the transmittance work described below. We also feel that in the future it should be possible to develop a higher spatial resolution night algorithm based on the absolute radiance.

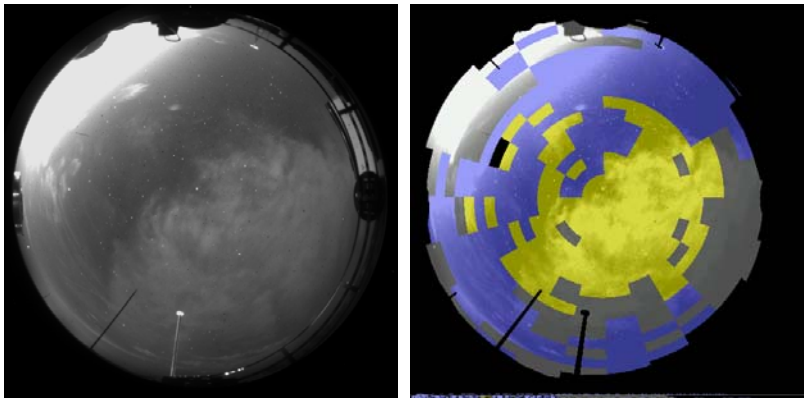

(a) (b)

Figure 4: Night algorithm results: a) Raw image; b) Cloud decision image.

Using these automated algorithms, it is possible to design systems that provide automatic alarms for unacceptable test conditions, and assess a variety of satellite tracks or other regions of the sky to make optimized test decisions. The data can also be used for studying CFLOS statistics and for other modeling efforts.

Another standard data product of the WSI is the absolute radiance distribution. Each pixel in the camera is calibrated, so the instrument provides approximately 180,000 measurements of radiance simultaneously. The systems are calibrated in each wave band. We are quite careful with the calibrations, measuring the impact of non-linearity, shutter opening time, non-uniformity, lens roll-off, pixel cross-talk, and so on. Absolute calibrations are traceable to NIST. A discussion of the calibration is beyond the scope of this paper, however the calibrations are generally self-consistent to within fractions of a percent. The lamps are accurate to 2-3%, depending on age, so we believe that the overall calibration is generally accurate to within 3 – 5%. At the present time, the sky radiance distributions are processed in archival mode, and are not an automated real-time product. Conversion to a real-time product, if an application required it, is straight forward.

The most recent data product is the distribution of earth-to-space beam transmittance over the night sky. Although a detailed development of the theory is beyond the scope of this paper, we can present an overview of the technique and the results. The 5th edition NSSDC Bright Star Catalog (Hoffleit, 1991) is used to determine the magnitude and color temperature of stars down to visual magnitude 7.96. From these values, the expected inherent irradiances of the stars in the WSI open hole passband are determined. By "inherent", we mean the effective irradiance of the stars above the atmosphere. A very accurate angular calibration of angle in object space vs. pixel position in image space enables a reasonably accurate determination of the association between the stars in the image, and the stars in the library. The images are calibrated for absolute radiance. We have found that the Point Spread Function of the atmosphere and the optics can be reasonably well described by a Gaussian with a width of 0.45 pixels over the full image. By integrating over this PSF and subtracting the background, we can make reasonably good determinations of the apparent irradiance of the stars in the image. By "apparent', we mean the irradiance as seen from the observer or WSI position. The ratio of apparent to inherent irradiance should yield the total earth-to-space beam transmittance.

Figure 5 shows the resulting relationship when the inherent and apparent star irradiances are compared. In this data set of 1555 stars of magnitude down to approximately 3.9, the correlation is very good, with a correlation constant of .968.

If stars down to a magnitude of approximately 7.0 are used, yielding a data set of nearly 33,000 stars for this night, the correlation is .847. We believe that this may be due to uncertainties in the star magnitude values. The ability of the WSI to observe the full upper hemisphere with a calibrated sensor simultaneously is a very strong capability, and should enable us to further improve the inherent star irradiance values.

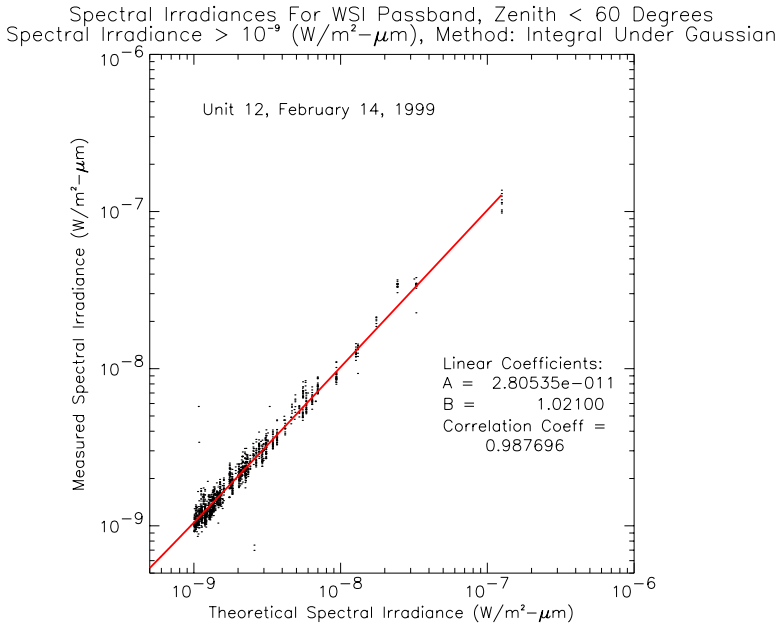

Figure 5: Observed relationship between the measured, or apparent star irradiance, and the computed, or inherent star irradiance on a clear night.

The resulting transmittance map is shown for a sample case in Figure 6. The raw data are shown in image a, and the total earth-to-space beam transmittance is shown in image b. For this plot, we used stars to magnitude 6.0 that were not too close to other stars. We determined from a series of clear nights that an earth-to-space beam transmittance of approximately 0.8 is typical for this filter; the residual transmittance corrected for the clear night transmittance is shown in image c. Although it is not obvious in this display of the raw data, there were clouds present in the bright band near the horizon. Although the variance in these results is somewhat higher than we would like, we are very pleased with this as a first result, and feel that it can be improved by modifying the inherent star values based on measurements on clear nights. Similar simultaneous measurements of the full star field in a variety of wavelengths from high altitude could be quite useful.

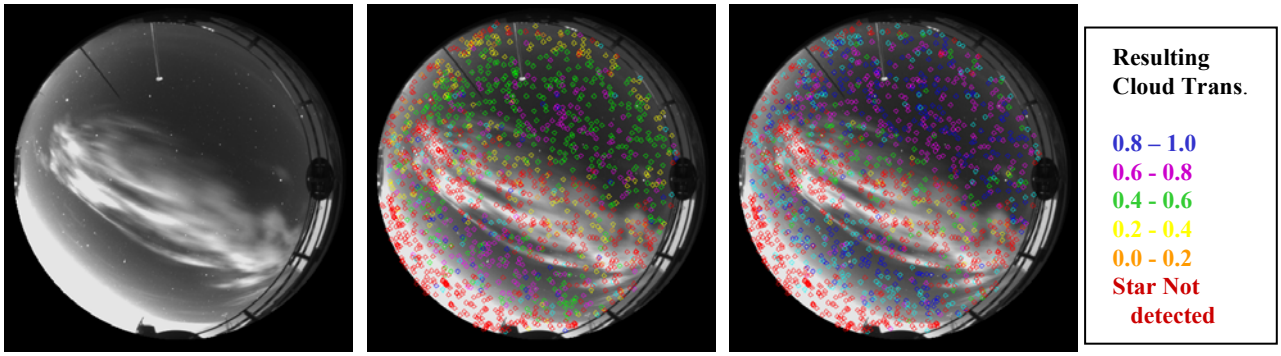

(a) (b) (c)

Figure 6: Transmittance Map Results: a) Raw data, b) the total earth-to-space beam transmittance result, c) the residual transmittance corrected for a clear-night vertical earth-to-space transmittance of 0.8.

4. CUSTOMIZED WSI'S FOR SPECIALIZED APPLICATIONS

Over the years, several versions of the WSI have been designed and deployed. This section will provide a very brief overview of these systems. Most of the WSI systems utilize cable bundles communicating between the controller and the sensor, and require that the sensor be within 230' of the controller. For the Day/Night WSI shown in Figure 7, the controller package was integrated into the sensor environmental housing. As a result, it can be sited remotely from the user. The WSI sends data via Ethernet link to a second computer, where data are processed in near-real time. The

computer can also accept instructions from another computer controlling another application or model. This computer can request moving regions of interest (ROI), and the WSI returns the information on cloud cover within this ROI to the user or model.

The original Day WSI developed in the 80's is obsolete, and a new version of the Day WSI has been developed based in part on the upgrades used in the Day/Night WSI systems. The Day WSI is shown in Figure 8, and an image near sunset (with the occultor nearly below the horizon) is shown in Figure 9. This system acquires imagery in seven user-selected passbands in the visible and NIR at approximately 1024 x 1024 resolution. It provides calibrated radiance distributions in all wavebands, as well as cloud fraction. This is the system for which a new daylight cloud algorithm is in development. It is further documented in Shields et al (2003 a). Like the Day/Night WSI, it provides high quality, fully shaded imagery appropriate for a variety of applications.

Figure 7: Day/Night WSI for Remote Sites

Figure 8: Day Visible/NIR WSI

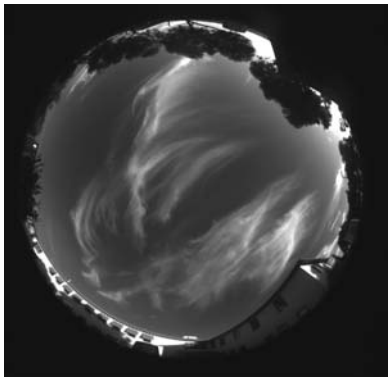

Figure 9: Raw image from Day WSI

A small calibrated fisheye imaging system has recently been developed for airborne use on a UAV. It consists of two camera packages, a visible system near 645 nm using Silicon CCD technology, and a NIR system near 1610 nm using InGaAs CMOS technology. The NIR camera and a visible image are shown in Figure 10. Both of the systems are fully calibrated, to provide the radiance distribution of the lower hemisphere, and the cloud top radiances in particular. Although this was designed for use with the ARM program, we feel that it has great potential for tactical and other military applications. This system is documented in Feister et al (2000) and Shields et al (2003b). We have also determined how we could develop similar systems at 3 –5 μm and 8 – 12 μm.

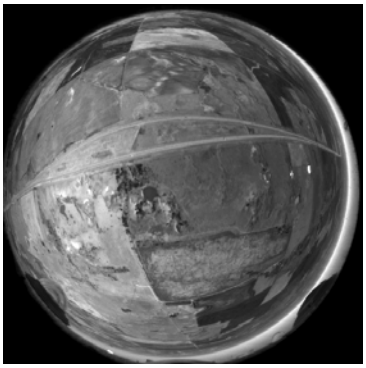

Figure 10: One of two airborne fisheye systems designed for use with a UAV. The first figure illustrates the camera that acquires images near 1.6 μm in the NIR, and the second image illustrates data from the visible system near 650 nm.

5. CLOUD FREE LINE OF SIGHT STATISTICAL STUDY

An early version of the Day WSI developed by MPL was fielded in the mid-to-late 1980's at several sites throughout the U.S., acquiring data once a minute for over two years. The data were originally acquired for support of ground-based high-energy laser applications, and approximately one year of data from each of several of the sites were processed through the cloud algorithm in those years. These processed data were recently further processed to extract statistics on Cloud Free Line of Sight (CFLOS) with funding from the Air Force's Starfire Optical Range. This section presents a sampling of the results extracted from this data set.

The processed data consisted of cloud algorithm results such as those shown in Figure 11. This was a fairly early version of the algorithm, but comparisons with observers over a limited test case showed very good agreement with the observer. Approximately 82,000 images such as given in Figure 11 were available at 10-minute intervals, and used for the CFLOS determinations. Approximately 820,000 images at 1-minute intervals were used for the Persistence studies.

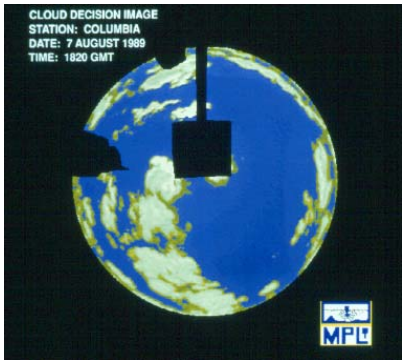

Figure 11: Sample Day WSI Cloud Algorithm Data Product for CFLOS Study

The PCFLOS data were extracted as a function of cloud fraction, zenith angle, station location, and season. Figure 12 shows some very preliminary data extracted from a limited sample of WSI data, in comparison with two models. The straight line "model", one minus cloud fraction, represents the relationship that might be expected if clouds were uniformly small, evenly distributed, and essentially had no physical thickness. If one takes into account the thickness of clouds, the result is similar to that shown by the curve labeled SRI model. These results were provided to us courtesy of TASC, Inc. The WSI data showed an interesting drop near 80% cloud cover. A more detailed study of the WSI, based on 24,000 cases near White Sands Missile Range (WSMR) shows the same behavior in Figure 13. We believe this behavior is real, and reflects the fact that clouds often are not evenly distributed small clumps. If the 80% cloud cover is associated with a front, and 80% of the sky is covered, then the zenith will also not be cloud free. This behavior is of course inverted near the horizon, as shown in the 75 degree zenith angle curve in Figure 13.

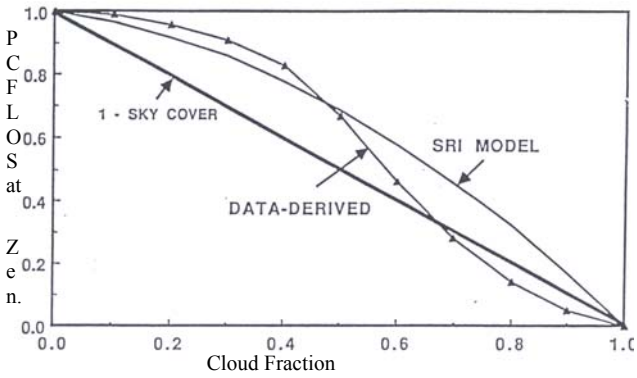

Figure 12: Model and Sample WSI Data for PCFLOS At the zenith as a function of Cloud Fraction.

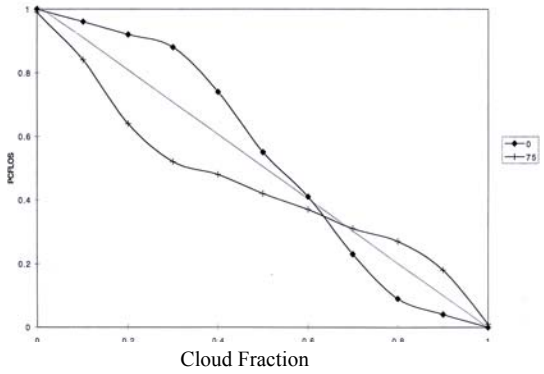

Figure 13: PCFLOS at Zenith and at 75 degrees zenith angle as a function of Cloud Fraction; data from WSMR, 24,000 cases.

Another type of data product extracted from the CFLOS data is the conditional probability. As an example, in Table 1 column 2, we show the probability that the sky is clear in the direction toward GOES-8, for each of 5 sites. These probabilities range from around 66% for the desert sites, to 35% for the coast of Florida. However, if we look at the conditional probility that the line of sight towards GOES-8 is clear given that the line of sight toward Polaris is clear, now the probabilities increase to 92% to 84%.

Table 1
Conditional Probability for a
Cloud Free Line of Sight to GOES-8

Location	PCFLOS in GOES-8 Direction	PCFLOS for GOES-8 if Polaris is clear
Albuquerque, NM	0.66	0.92
White Sands, NM	0.63	0.90
Columbia, MO	0.46	0.86
Malmstrom AFB, MT	0.38	0.72
Malabar Tracking Station, FL	0.35	0.84

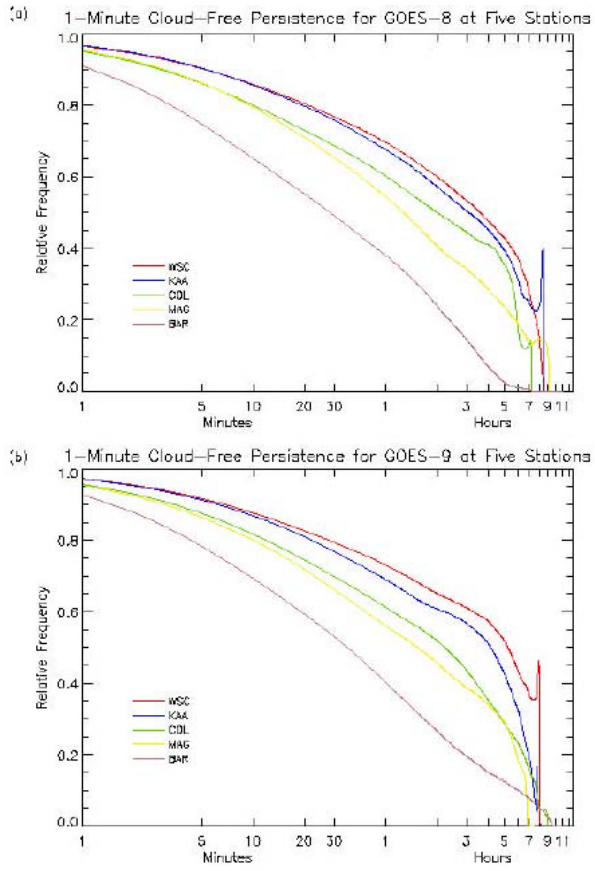

Figure 14: Cloud-free Persistence results for yearly Averages at five stations and in two directions.

It is also interesting to evaluate the persistence. Figure 14 shows a sample persistence result. For those cases which had a clear line of sight in a given direction at Time T_0, we determined what fraction of these cases remained clear throughout the interval from time T_0 to time T. The upper plot shows five stations for the GOES-8 direction, and the lower plot shows the GOES-9 direction. At some of the stations, such as those in the desert, the probability of persistence was quite high. For example, at WSMR, the probability fell to 50% only after over 5 hours. At the Florida site, the probability fell to 50% after less than an hour. Similar studies were made as a function of season, and also studies of the persistence of cloudy conditions were made. These results are shown in Table 2.

Table 2
Persistence Results:
Time (hr) Required for Yearly Persistence
Probabilities for Polaris to drop below 0.5

Location	Cloud-free	Cloudy
Albuquerque, NM	4.1	1.1
White Sands, NM	5.1	0.7
Columbia, MO	3.1	2.6
Malmstrom AFB, MT	1.5	2.9
Malabar Tracking Station, FL	0.8	0.4

In Table 2, the persistence of cloud-free conditions is quite long for the desert sites, and shorter for the other sites, as expected. The persistence of cloudy conditions is short for the desert sites. For the first four sites in the table, the cloudy persistence increases, as the cloud-free persistence decreases. However, for the coastal Florida site, where we often seemed to observe small fast-moving clouds, both the cloud-free and cloudy persistences were short.

While the above CFLOS and Persistence data give a small sampling of the type of statistics that were extracted from the WSI data-base, there are many statistics that can be extracted. For example, we evaluated multi-station behavior, in terms of both CFLOS and Persistence, and conditional probabilities such as the time persistence for having N stations with a clear line of sight, if M stations were available.

6. A TACTICAL FULL SCENE IMAGER (PATENT PENDING)

Another development that has come out of the Whole Sky Imager family of systems is the concept for a Tactical Full Scene Imager. In its simplest concept, this system uses a single fisheye lens with a beam splitter behind the lens to create two image planes, as shown in Figure 15. One of the image planes is used to provide an image of the full hemisphere scene, either using a tapered fiber optic bundle as shown, or using a lens, or by using imaging directly onto a chip if feasible. The second image plane is interrogated with a microscope objective, in order to provide a high-resolution view of a portion of the scene.

This concept is demonstrated in Figures 16 and 17. Figure 16 shows the full fisheye view (180 degrees in field of view) of the test room. Image (a) has been displayed to show the room, and image (b) has been displayed to show the optical target.

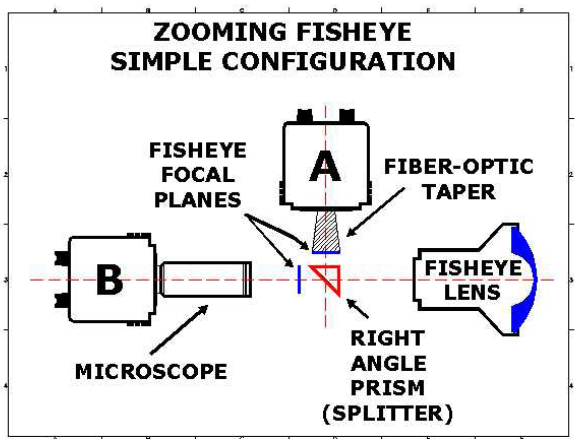

Figure 15: The simplest concept for the Tactical Full Scene Imager concept

Figure 17 shows the image through the microscope objective. The image plane has a high spatial frequency content, well beyond that which is acquired in the imagery shown in Figure 16. As a result, it is possible to extract high resolution imagery with a behind-the-lens optical zoom using a microscope objective. Image (b) of Figure 17 shows a small portion of image (a) further enhanced using electronic zoom. Image (c) of Fig. 17 shows the best we could achieve with electronic zoom alone.

(a) (b)

Figure 16: Image of the full scene in a test room: a) displayed to show the room, b) displayed to show the target

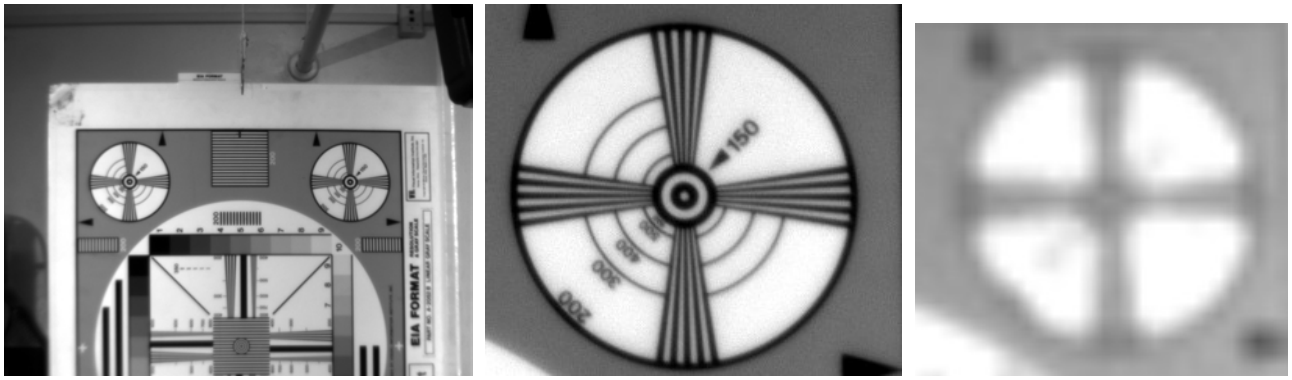

(a) (b) (c)

Figure 17: Images using Zooming: a) Image of the image plane through a microscope, b) Image of the target using both optical and Electronic zoom, c) Image of the target using electronic zoom alone.

This concept could be used with human interaction, or could be fully automated. For example, a human in a tank could view an image such as in Figure 16, chose an area of interest using a touch-screen monitor, and the system could display the high resolution view of the selected area of interest. Similarly, a motion detection algorithm could be used to automatically select the area of interest. A number of different lens and camera configurations is possible. For example, use of three fisheye lenses would enable the full spherical surround to be viewed continuously with a completely staring system. The system should be far more robust, dust-resistant, and covert in comparison with external optical zoom, and we have developed methods for doing very fast changes to the region of interest. The system currently has a patent pending, and is in mock-up stage. We feel that it has many applications both for tactical applications in unattended ground sensors, tanks, and ships, as well as for now-casting in the battlefield environment.

7. SUMMARY

The Whole Sky Imagers have been developed for a number of applications, including military and general research applications. The data products can include the raw images, cloud decision images, and absolute radiance distributions. More recently the ability to determine the distribution of beam transmittance over the full sky at night has been developed but not yet integrated into the real-time processing software. Several versions of the instrument have been developed, including a Day/Night WSI, Day/Night WSI with automated real-time processing, Day WSI, and an airborne fisheye system. Cloud Free Line of Sight statistics have been extracted from part of the WSI data base. Concepts for tactical systems and now-casting are in development.

8. ACKNOWLEDGEMENTS

We would like to express our appreciation to the Starfire Optical Range, for their support of much of this work, as well as for providing partial support to enable the presentation of these results. We would especially like to thank Ann Slavin for her advice and technical support in this work. In addition, we would like to thank Dr. Tim Tooman at Sandia National Laboratories, and the DOE's Atmospheric Radiation Measurements Program administered by Battelle's Pacific Northwest National Laboratories, for their support of much of the D/N WSI development. Thanks also to the Air Force Research Labs, and to Deutsche Wetterdienst, the German Weather Service which supported some aspects of the research. We would like to recognize Roper Scientific, for their assistance with the Photometrics camera products.

9. REFERENCES

1. R. W. Johnson, W. S. Hering, and J. E. Shields, *Automated Visibility and Cloud Cover Measurements with a Solid State Imaging System*, University of California, San Diego, Scripps Institution of Oceanography, Marine Physical Laboratory, SIO 89-7, GL-TR-89-0061, NTIS No. ADA216906, 1989.

2. J. E. Shields, R. W. Johnson, and T. L. Koehler, *Automated Whole Sky Imaging Systems for Cloud Field Assessment*, Fourth Symposium on Global Change Studies, American Meteorological Society, 1993.

3. J. E. Shields, R. W. Johnson, M. E. Karr, and J. L. Wertz, *Automated Day/Night Whole Sky Imagers for Field Assessment of Cloud Cover Distributions and Radiance Distributions*, Tenth Symposium on Meteorological Observations and Instrumentation, American Meteorological Society, 1998.

4. R. W. Johnson, W. S. Hering, J. I. Gordon, B. W. Fitch, and J. E. Shields, *Preliminary Analysis and Modeling Based Upon Project OPAQUE Profile and Surface Data*, University of California, San Diego, Scripps Institution of Oceanography, Visibility Laboratory, SIO Ref. 80-5, AFGL- TR-0285, NTIS No. ADB-052-1721, 1980.

5. Hoffleit, E.D., and W.H. Warren Jr., *The Bright Star Catalogue.* 5th ed. New Haven,Conn.: Astronomical Data Center and Yale University Observatory, 1991.

6. Feister, U., Shields, J., Karr, M., Johnson, R., Dehne, K. and Woldt, M, *Ground-Based Cloud Images and Sky Radiances in the Visible and Near Infrared Region from Whole Sky Imager Measurements*, Proceedings of Climate Monitoring – Satellite Application Facility Training Workshop sponsored by DWD, EUMETSAT and WMO, Dresden 2000.

7. J. E. Shields, R. W. Johnson, M. E. Karr, A. R. Burden, and J. G. Baker, *Daylight Visible/NIR Whole Sky Imagers for Cloud and Radiance Monitoring in Support of UV Research Programs*, International Symposium on Optical Science and Technology, SPIE the International Society for Optical Engineering, 2003a.

8. J. E. Shields, R. W. Johnson, M. E. Karr, A. R. Burden, and J. G. Baker, *Calibrated Fisheye Imaging Systems for Determination of Cloud Top Radiances from a UAV*, International Symposium on Optical Science and Technology, SPIE the International Society for Optical Engineering, 2003b.